Use of spectral gamma-ray signature to interpret stratigraphic surfaces in carbonate strata: An example from the Finnmark carbonate platform (Carboniferous–Permian), Barents Sea

S. N. Ehrenberg and T. A. Svånå

ABSTRACT

Spectral gamma-ray (GR) profiles were examined in well 7128/6-1, the stratigraphic reference section of the entirely subsurface Finnmark carbonate platform. Detailed bulk-chemical profiling of selected GR peaks shows that potassium (K) and thorium (Th) are mutually correlated and are a direct index of siliciclastic (aluminosilicate) content, whereas uranium (U) is uncorrelated with K, Th, and all other chemical components measured. Uranium tends to be enriched in thin shale and argillaceous carbonate layers within otherwise carbonate-dominated intervals. Uranium is thus associated with aluminosilicate minerals and is not particularly concentrated in dolomite. Two types of GR peaks are observed. Potassium-thorium–dominated peaks are suggested to indicate relatively major transgressions during which aluminosilicate detritus was derived from sources interior to the Fennoscandian shield. Uranium-dominated peaks correspond with relatively minor transgressions within intervals of cyclic shallow-water carbonate deposits. Uranium-enriched aluminosilicate detritus is suggested to be the product of extended subaerial exposure of the platform, during which U was concentrated by groundwater movement. These results can be useful as a basis for applying spectral GR signature as a tool for stratigraphic interpretation in uncored or incipiently understood carbonate sections.

Manuscript received August 25, 1999; revised manuscript received March 23, 2000; final acceptance June 30, 2000.

AUTHORS

S. N. Ehrenberg ~ *Statoil, N-4035 Stavanger, Norway; sne@statoil.com*

Steve Ehrenberg has a Ph.D. from University of California–Los Angeles. He joined Statoil in 1985, where he does technical service projects in clastic and carbonate petrology. In between there is time for the occasional scientific article.

T. A. Svånå ~ *Statoil, Postboks 40, N-9401 Harstad, Norway; tasv@statoil.com*

Tore Svånå received his Candidatus Scientiarium degree in geology (sedimentology) at the University of Oslo in 1984. He began his professional career as well site/operations geologist, first at Norsk Hydro and thereafter at Statoil. He has worked mainly on Barents Sea exploration, with particular emphasis on Upper Paleozoic carbonates. He has also been involved in the evaluation of Mideast opportunities, was the leader for Statoil's former carbonate research program, and has co-authored several publications.

ACKNOWLEDGEMENTS

Helpful suggestions on the manuscript were contributed by L. Stemmerik, E. G. Purdy, and AAPG referees J. H. Doveton, S. C. Ruppel, and T. Elliott.

INTRODUCTION

The natural gamma radiation of rocks is the composite of emissions produced by isotopes of potassium (K), thorium (Th), and uranium (U) (Dypvik and Eriksen, 1983). The relative contributions of these elements to the total gamma ray (GR) log profile of a bore hole can be differentiated by a spectral GR logging tool, and such patterns are commonly examined in hydrocarbon exploration wells as a means of estimating mineralogy, differentiating depositional environments, and recognizing significant stratigraphic surfaces (Schlumberger, 1982; Davies and Elliott, 1996; North and Boering, 1999). For carbonate strata, however, rather few studies documenting spectral GR significance have been published, although there appears to be widespread appreciation that K and Th reflect clastic content, whereas U is determined by diagenetic processes involving changes in oxidation state (for example, Lucia, 1999, p. 62–63). Most of the published carbonate spectral GR studies ascribe localized U enrichment to movements of late diagenetic fluids (Hassan et al., 1975; Fertl et al., 1980; Luczaj, 1998).

The present article reports observations from an exploration well where spectral GR log patterns in carbonate strata appear to have a distinctive relationship to depositional facies and stratigraphic surfaces. A program of detailed analysis of several intervals containing prominent GR peaks was undertaken because it was realized that the recurrent spectral GR patterns associated with these peaks could yield general knowledge useful for interpreting stratigraphic relationships elsewhere. This article is part of a larger effort to provide detailed petrologic information on the Carboniferous–Permian Finnmark carbonate platform, as a basis for seismic interpretation and prospect evaluation (Ehrenberg et al., 1998a, b; 2000a, b).

STRATIGRAPHIC SETTING

Petrologic studies have focused on well 7128/6-1 (Figure 1), which is regarded as the stratigraphic reference section for the Finnmark carbonate platform because of its extensive core coverage (445 m of the 527 m Upper Carboniferous through Upper Permian succession) and the relatively complete stratigraphy preserved in this location. Detailed sedimentologic and diagenetic description of the 7128/6-1 section is provided in Ehrenberg et al. (1998a, b). They define nine lithostratigraphic units (L-1 to L-9), which are interpreted as comprising seven major depositional sequences (S-1 to S-7) and numerous higher frequency transgressive-regressive cycles (Figure 2). Formal stratigraphic nomenclature has been proposed for upper Paleozoic strata of the Barents Sea subsurface (Larssen et al., 1999), but detailed application to individual well sections remains uncertain and is not attempted here.

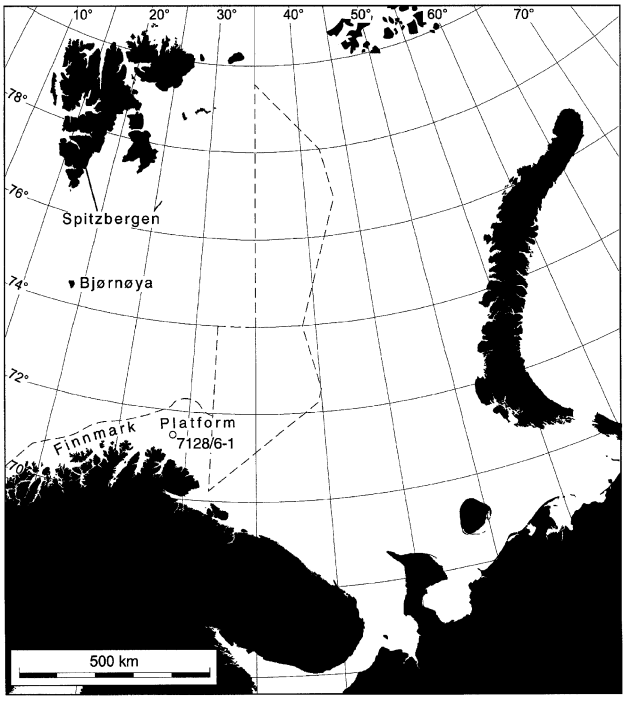

Figure 1. Map of the Barents Sea, showing well location, boundary of Finnmark Platform, and zone of boundary dispute between Norway and Russia (thin dashed lines).

In the Late Carboniferous through the Permian, the Barents Sea was part of a vast province of carbonate-dominated deposition that extended from the Canadian arctic to northern Russia and thence southward to the Caspian Sea (Stemmerik and Worsley, 1995). The Finnmark carbonate platform is a segment of this province that is bounded to the south by the erosional subcrop onto the Fennoscandian craton and to the north by a sharp increase in depositional paleoslope, where platform carbonates pass laterally into evaporites and deep-water facies of the Nordkapp Basin.

Following extension tectonism and accumulation of thick siliciclastic units in the Early Carboniferous (Visean), the Finnmark carbonate platform underwent four distinct stages of depositional evolution, which are correlated to the 7128/6-1 section as shown at the right margin of Figure 2. These stages

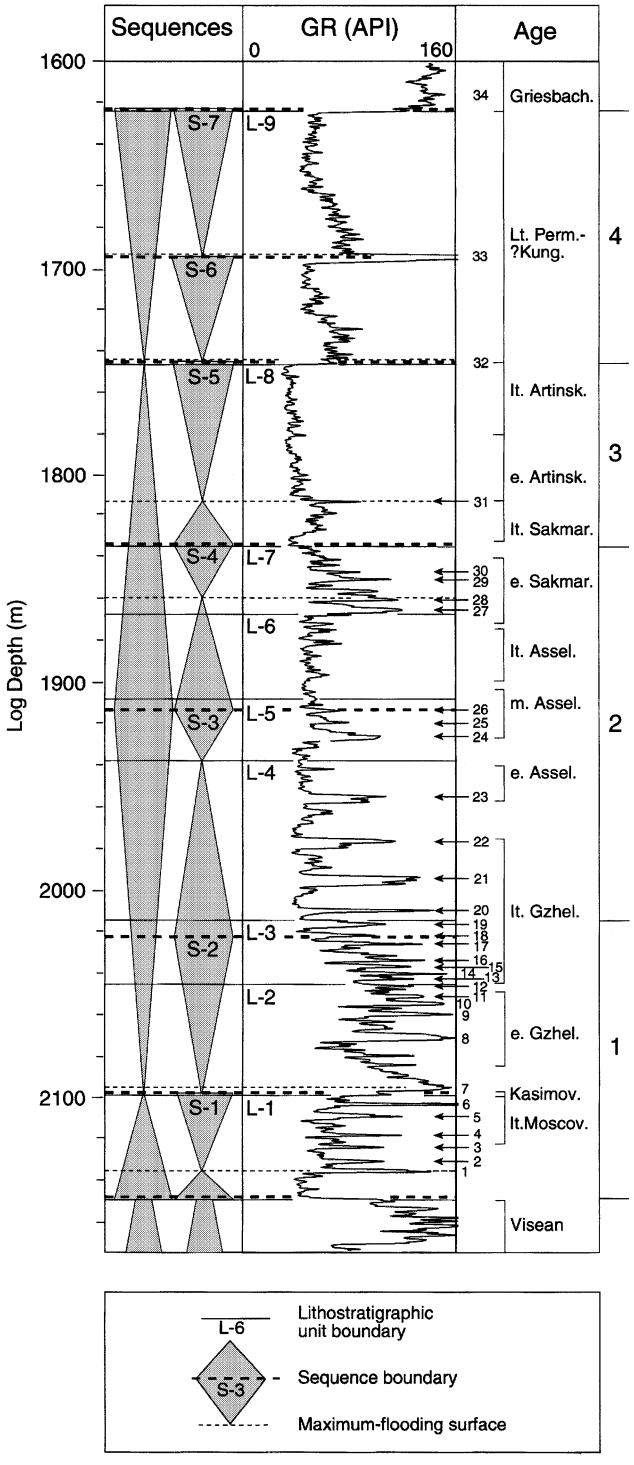

Figure 2. Sequence stratigraphic interpretation, GR profile, and age constraints of the Upper Carboniferous–Permian succession in well 7128/6-1. Sequences S-1 through S-7 are major (possibly third-order) depositional sequences defined by Ehrenberg et al. (1998a). These make up a larger scale (second-order) cyclicity indicated at left. Tops of lithostratigraphic units (L-1 through L-9) are labeled to left of GR trace. The GR peaks examined are numbered 1–34. Numbers at right margin indicate four stages of platform evolution.

include (1) Late Carboniferous mixed siliciclastic-carbonate deposits, reflecting waning tectonic influence; (2) latest Gzhelian through early Sakmarian cyclic warm-water carbonates containing frequent algal buildups and abundant dolomite and anhydrite; (3) late Sakmarian through Artinskian cool-water carbonates, including crinoid-bryozoan grainstones to wackestones in the 7128/6-1 location and major bryozoan mud mounds nearer the platform margin; (4) Kungurian–Late Permian cold-water spiculite, carbonate, and siliciclastic deposits, abruptly terminated by massive siliciclastic influx in the earliest Triassic. As discussed by Beauchamp and Desrochers (1997), for the broadly equivalent strata of arctic Canada, replacement of photozoan biota by progressively cooler water heterozoan biota from stages 2 through 4 records cooling along the northern margin of Pangea, probably due to changes in oceanic circulation patterns.

The 7128/6-1 cores were described by Ehrenberg et al. (1998a) using a system of 12 broadly defined microfacies (Figure 3), including one category for *Palaeoaplysina* and phylloid algae buildups (embracing the complete spectrum from wackestone to grainstone to bafflestone). Numerous exposure surfaces are believed to be present throughout units L-1 through L-7 because these shallow-water carbonates were deposited during a time of large-amplitude, high-frequency sea level fluctuations (Veevers and Powell, 1987). Outcrop studies of equivalent strata from Svalbard (Pickard et al., 1996; Stemmerik and Larssen, 1993) demonstrate that exposure surfaces typically show great lateral variation in the degree of development of various exposure criteria, such that recognition of such surfaces in one-dimensional core studies is likely to be problematic. Although exposure surfaces have been inferred at specific locations in the cores, all of these surfaces are to varying degrees ambiguous, and any of them could alternatively be explained as the product of submarine erosion or cementation (Shinn, 1986).

A hierarchy of depositional sequences has been defined in the 7128/6-1 section based on patterns of variation in facies and cycle thickness. The carbonate platform succession is divisible into two largest scale depositional sequences (Figure 2) spanning the late Moscovian to Late Permian. Each of these supersequences includes three to four major sequences (designated S-1 through S-7; Figure 2), having average durations of 7–9 m.y. but much wider limits on their individual age constraints (<1–22 m.y.).

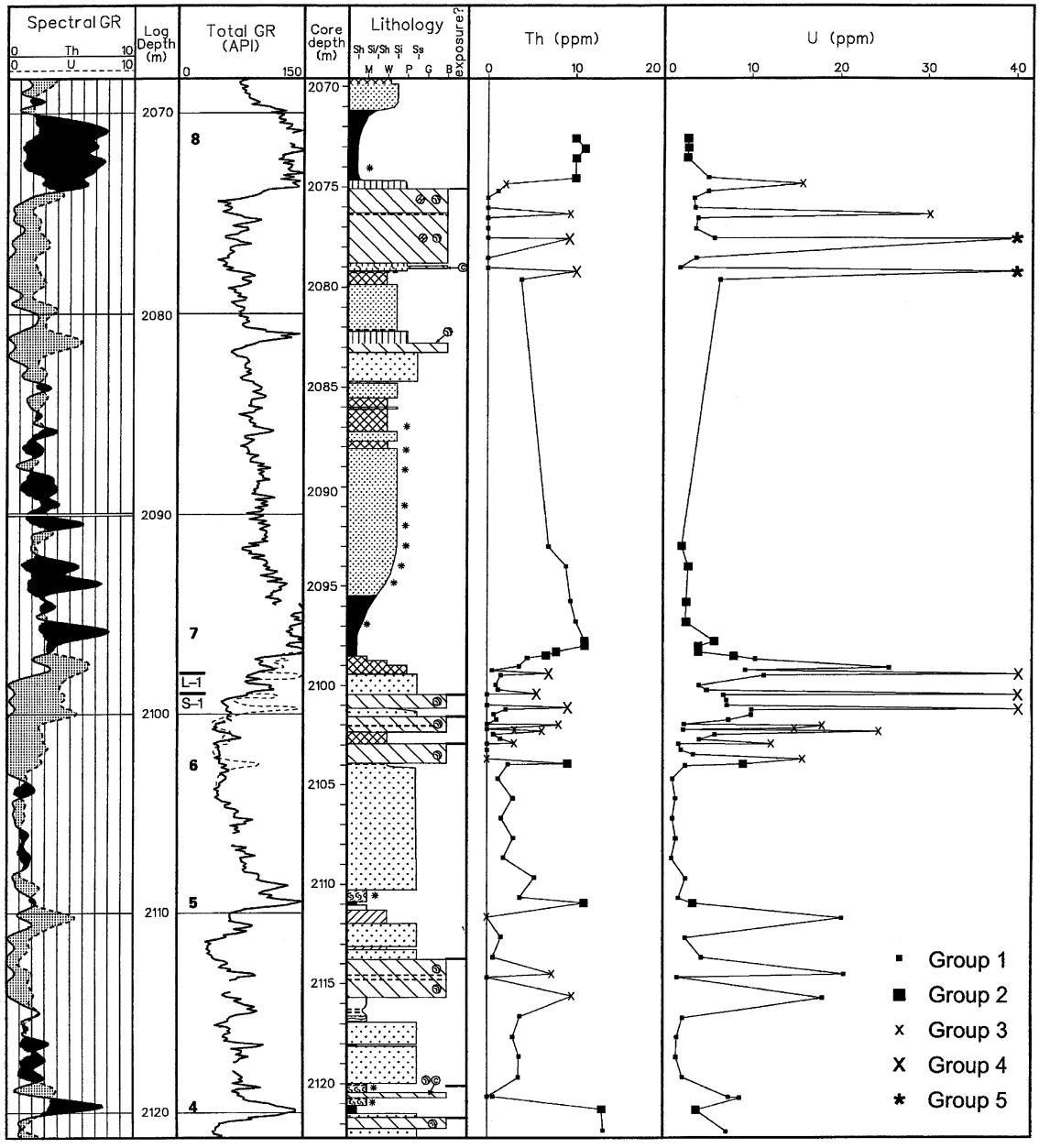

Fill pattern between Th and U curves (ppm units):

- Th > U
- U > Th

Lithology:

- Bryozoan-crinoid grain/packstone
- Bryozoan-crinoid wackestone
- Foraminifera grain/packstone
- Fusulinid wacke/packstone
- Barren dolomitic mudstone
- Laminated dolomitic mudstone
- Bioturbated dolomitic mudstone
- Buildup
- Sandstone
- Calcareous siltstone
- Shale
- Shale layers (mainly 1-5 cm thick)
- Glauconite

Figure 3. Spectral GR profiles of U and Th in upper part of unit L-1 and lower L-2 compared with total-GR log, lithologic description of cores, and bulk chemical analyses of U and Th. The GR peak numbers (from Figure 2) and tops of lithostratigraphic unit L-1 and of sequence S-1 are indicated at left side of total-GR track. Total-GR profile recorded from slabbed core surface (dashed curve from 2098 to 2105 m) shows more detail than wire-line GR log (solid curve). Plotting symbols in right-hand columns indicate sample groupings defined in Figure 7.

ANALYTICAL TECHNIQUES

Careful attention has been given to accurate correction between core depth (CD) and log depth (LD). These corrections are substantial in many places, and one 16 m interval of the core (2005.25–2021.60 m CD) was even found to have been mistakenly turned upside down in the course of handling. Depth shifts were determined mainly based on comparison between the GR logs run in the well and along the surface of the core before slabbing. Additional adjustments of up to 1 m, however, were found to be necessary for several intervals where a second GR profile was run along the slabbed surface of the viewing cut of the core.

Wire-line logging of well 7128/6-1 was done by Western Atlas International. Only the spectral U and Th curves were used in the present study because the spectral K curve appeared to have relatively low sensitivity, possibly due to the use of KCl polymer mud, and the bulk chemical data demonstrated linear correlation between Th and K, such that K variations are implicit in the spectral Th curve.

Bulk chemical analyses were performed at fixed 1 m spacing over most of the cored intervals and at closer spacing around GR peaks selected for study. All analyses were done by XRAL, Ontario, Canada, using techniques described in Ehrenberg and Siring (1992).

SPECTRAL GR PATTERNS

Prominent GR peaks in the Moscovian–Upper Permian section of well 7128/6-1 are numbered 1–34 from the base of the section upward (Figure 2). Three intervals within the Moscovian–Sakmarian part of the section (units L-1–L-7) were studied in detail (Figures 3–5). To simplify the display of the spectral GR data, variations in K abundance have been assumed to be implicit in the Th curve. This assumption is justified by the strong linear correlation observed between K and Th in the bulk chemical analyses (Figure 6A). Only in one thin interval (discussed subsequently) is there any marked departure from this correlation.

The GR peaks can be divided into two general types based on relative spectral GR intensities.

K-Th–Dominated Peaks

The K-Th–dominated peaks occur in lithostratigraphic units L-1, L-2, and L-7. Most of these peaks appear to be composite, consisting of a U-rich (high-U/Th) lower part having minor to moderate total GR intensity, overlain by a K-Th–rich (low-U/Th) upper part having much greater total GR intensity. Several of these composite GR peaks correspond to sequence or cycle boundaries where transgressive shales overlie suspected exposure surfaces.

The best example of this is GR peak 7, which coincides with the top of sequence S-1 (Figure 3). This surface is interpreted as an unconformity based partly on truncational geometries visible on seismic and correlated to this approximate level in the well. Whether any section has been lost by erosion in the well location, however, is unknown. Fusulinid datings indicate a hiatus at this surface because unit L-1 is of late Moscovian age and the basal bed of unit L-2 (at 2099 m core depth) is middle Kasimovian (Figure 2). The top of unit L-1 (corresponding to the U-rich lower part of GR peak 7) consists of thin cycles of sandstone and phylloid algal buildups capped by apparent exposure surfaces (2099–2105 m). The bulk chemical analyses show that the high-U/Th GR response of this interval results from the cumulative contributions of numerous thin (generally <20 cm) argillaceous carbonate beds and even thinner (<5 cm) layers of black shale within thicker (0.2–1 m) carbonate beds having generally low radioactivity (Figure 3). The low-U/Th upper part of GR peak 7 (2093–2099 m) corresponds to an upward-coarsening interval of shale to shaly siltstone at the base of unit L-2. The lower meter of this interval is interpreted as containing the maximum flooding surface of sequence S-2, immediately overlying the S-1 sequence boundary (Figure 2).

Similar relationships are observed for GR peak 8, where several meters of low-U/Th transgressive shale overlie an inferred exposure surface (cycle top) at 2075 m, developed at the top of a phylloid algal-*Palaeoaplysina* buildup containing thin high-U/Th shale seams (Figure 3). The overlying GR peaks 9–11 in the upper part of unit L-2 have similar spectral GR characteristics, but are not shown in the figures presented here because this interval is not covered by bulk chemical analyses of U and Th.

Gamma-ray peak 27 in the lower part of unit L-7 also has a composite spectral GR pattern (Figure 5) that has a dominant K-Th–rich upper zone (1864–1866 m) and a subordinate U-rich lower zone (1866–1868 m). The overlying GR peak 28 appears to have a simple K-Th–rich spectral GR log profile, but the bulk chemical analyses reveal that this peak also rests

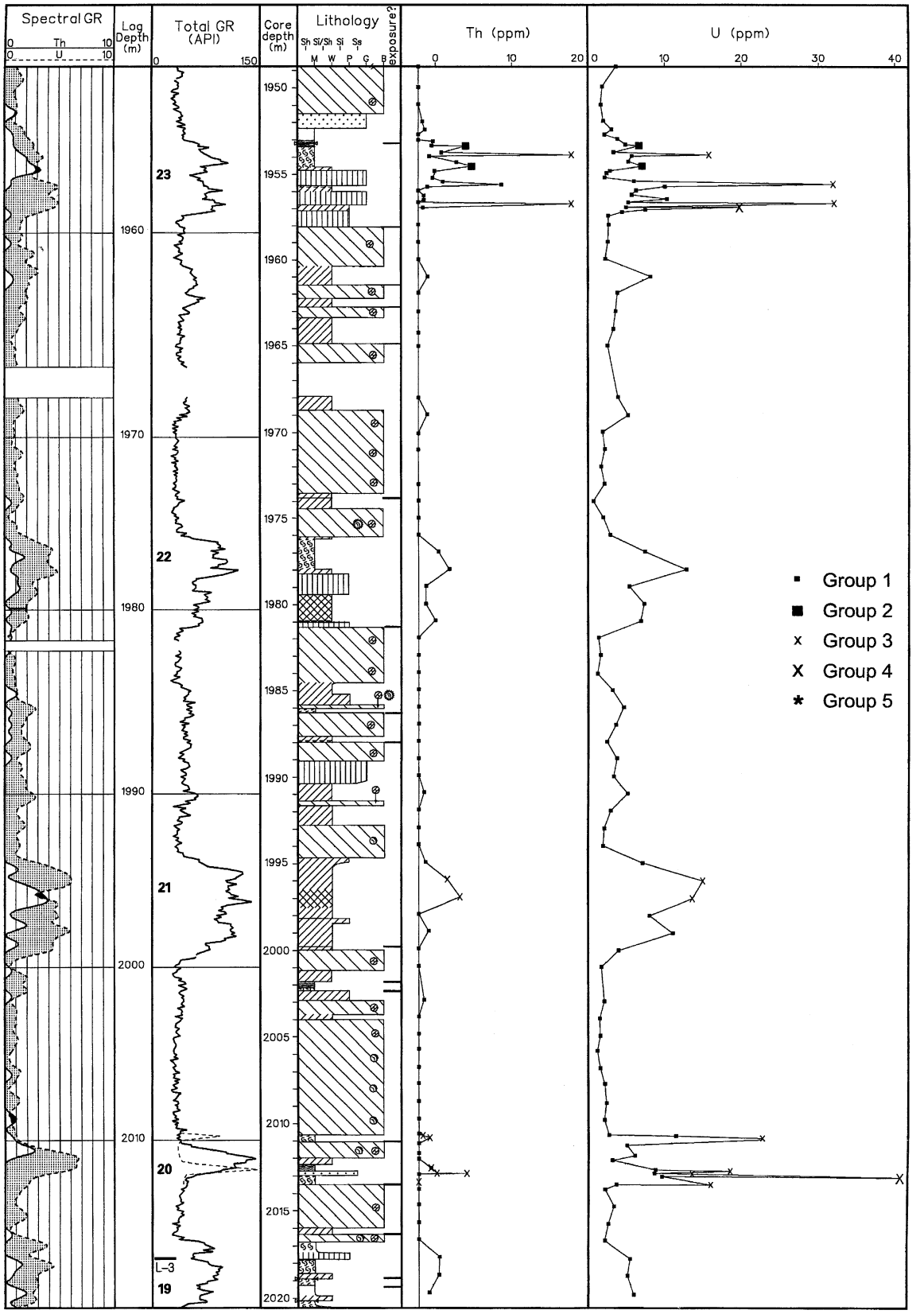

Figure 4. Spectral GR profiles of U and Th in lower part of unit L-4 compared with total-GR log, lithologic description of cores, and bulk chemical analyses of U and Th. Total-GR profile recorded from slabbed core surface (dashed curve from 2010 to 2013 m) shows more detail than wire-line GR log (solid curve). Plotting symbols in right-hand columns indicate sample groupings defined in Figure 7. In the "Th (ppm)" column, two points that have Th $>$ 20 ppm (group 5) are plotted with Th $=$ 20 ppm. See Figure 3 for explanation of lithology symbols.

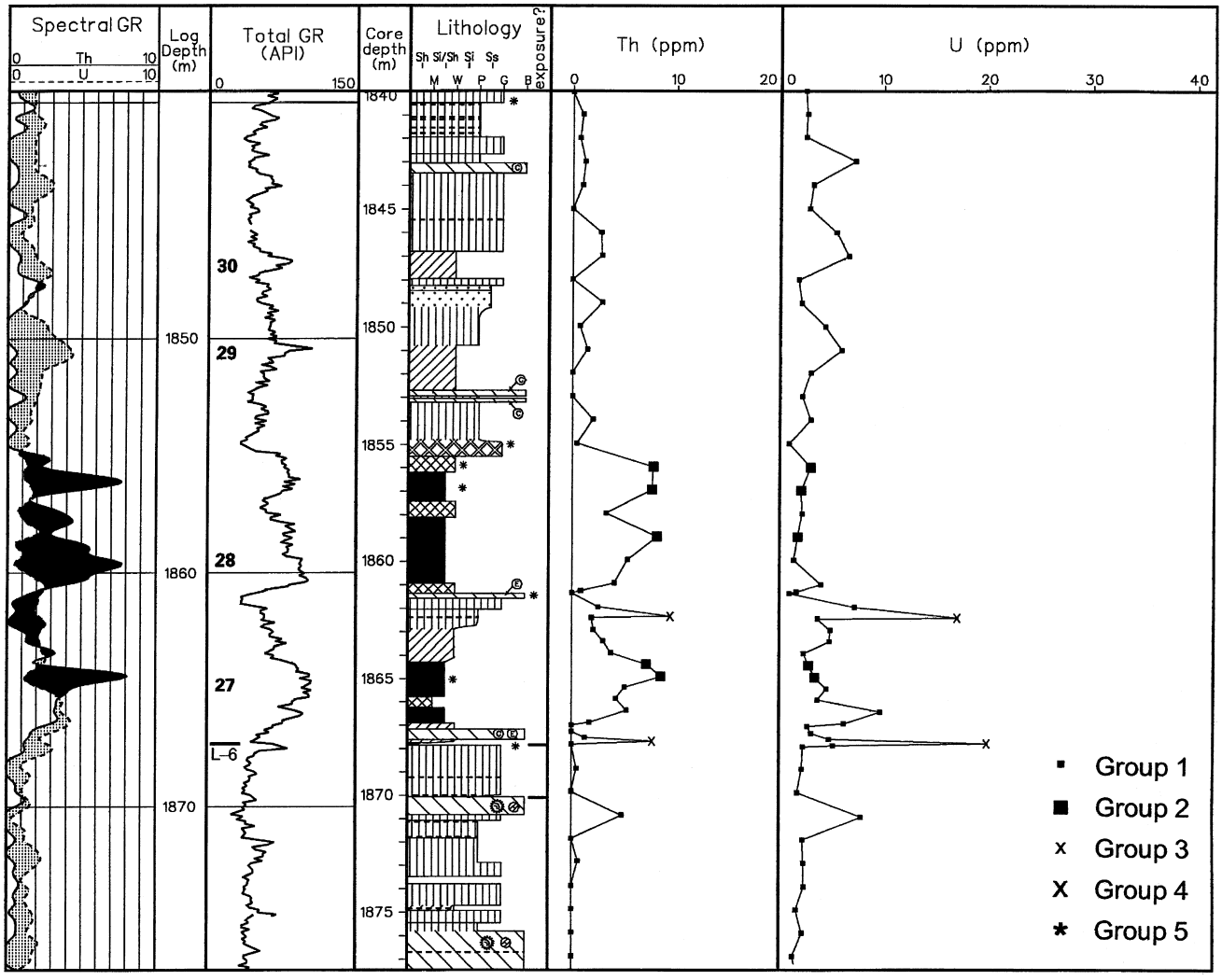

Figure 5. Spectral GR profiles of U and Th in upper part of unit L-6 and most of unit L-7 compared with total-GR log, lithologic description of cores, and bulk chemical analyses of U and Th. Plotting symbols in right-hand columns indicate sample groupings defined in Figure 7. See Figure 3 for explanation of lithology symbols.

upon limestones that have thin U-rich zones. Gamma-ray peaks 27 and 28 are interpreted as marking major fluctuations in relative sea level, based on the abrupt facies shifts from exposure-capped shallow-water limestones to deep-water calcareous shale (Ehrenberg et al., 1998a). These twin GR peaks are recognizable in other wells over large areas of the Barents Sea, suggesting that these transgressions may reflect important eustatic events rather than fluctuations driven by local tectonics.

Gamma-ray peaks 31–34 in units L-8 and L-9 (Figure 2) are not the focus of this article; all have spectral Th intensity greater than or equal to spectral U intensity.

U-Dominated Peaks

The U-dominated peaks mostly occur in lithostratigraphic units L-3 through L-7 (peaks 12–26; Figure 6, and peaks 29–30; Figure 7). These peaks are U-rich throughout, but several include a subordinate, moderately K-Th–rich zone. The U-dominated GR peaks correspond with intervals of clay-rich (marly) carbonate interpreted as the transgressive part of high-frequency transgressive-regressive cycles of carbonate deposition (Ehrenberg et al., 1998a). An example of such a cycle is the interval from 1981 to 2000 m in Figure 4. The U-rich lithologies are mainly fusulinid wackestones to fossiliferous mudstones containing

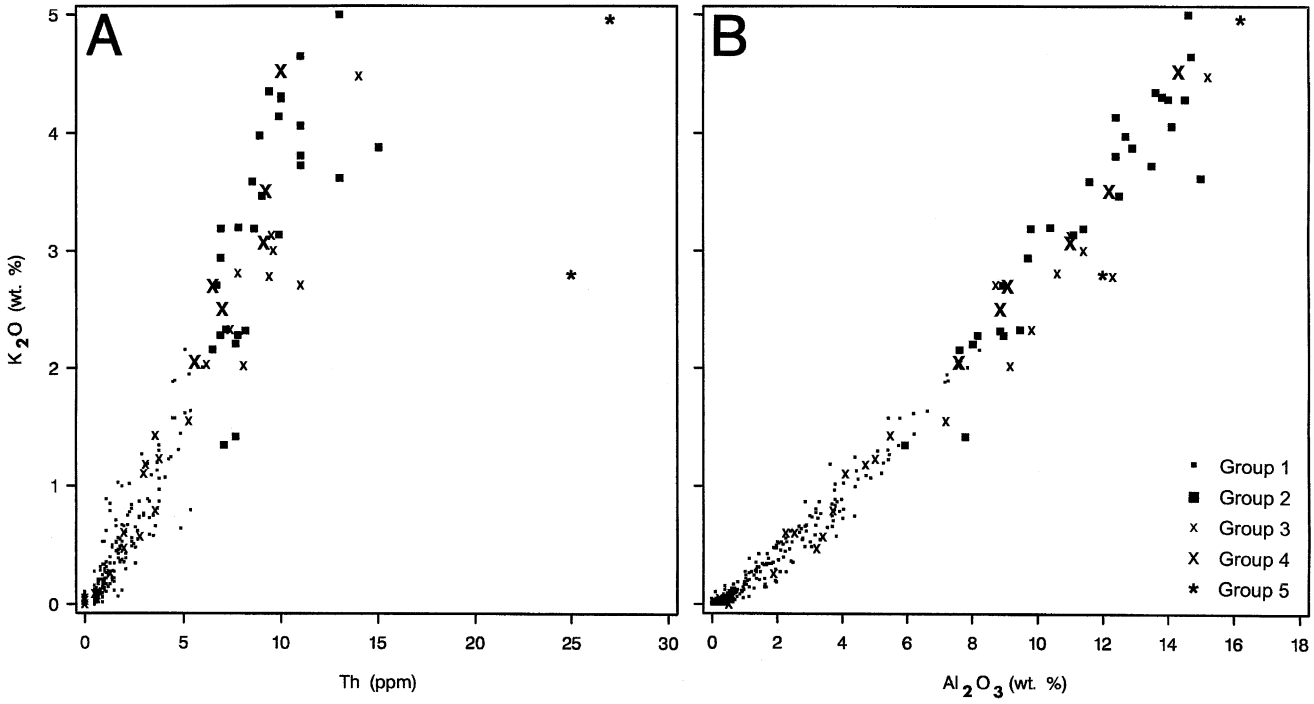

Figure 6. Bulk-rock K vs. (A) Th and (B) alumina in Moscovian through Upper Permian samples (units L-1 through L-9) from well 7128/6-1. Plotting symbols indicate sample groupings defined in Figure 7.

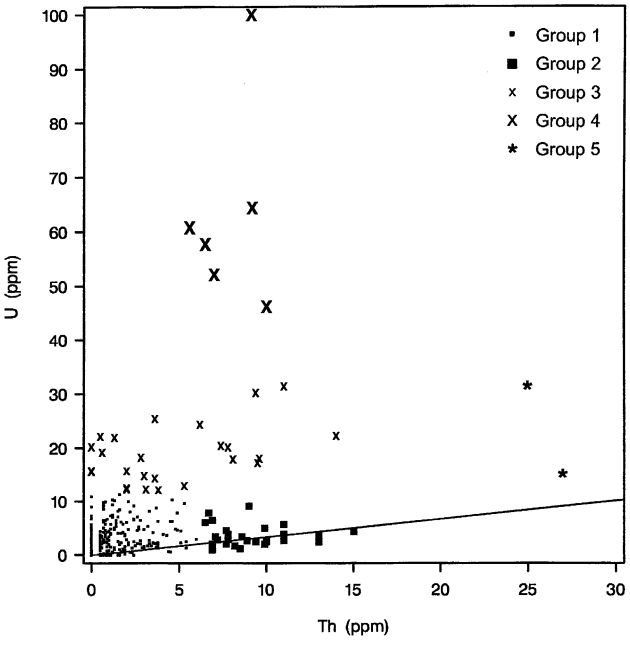

Figure 7. Bulk-rock U vs. Th in Moscovian through Upper Permian samples (units L-1 through L-9) from well 7128/6-1. Plotting symbols indicate the five fields of U vs. Th content shown here (described in text). The diagonal line illustrates Th/U = 3, suggested to be a minimum detrital value for shales that have not experienced authigenic enrichment in U (Myers and Wignall, 1987).

abundant argillaceous laminations. The degree of dolomitization of the U-rich intervals is widely variable but generally low (the dolomitization log is presented in Ehrenberg et al., 1998a).

BULK CHEMICAL COMPOSITIONS

Abundances of K, Th, and aluminum (Al) are mutually correlated in these Carboniferous–Permian strata (Figure 6), as has been observed previously in other studies (Hassan et al., 1976; Schlumberger, 1982). Uranium is uncorrelated with K, Th, and all other components measured, but it tends to be enriched in thin shale layers having moderate to high K, Th, and Al (Figure 7). Low-alumina carbonate rocks immediately adjacent to these thin U-rich shale layers tend to have low contents of both U and Th, although a subordinate group of these samples has moderate U contents (12–25 ppm) (Figure 7).

Based on U and Th abundances (Figure 7), the bulk chemical analyses were subdivided into five groups (identified by plotting symbols in Figures 3–9):

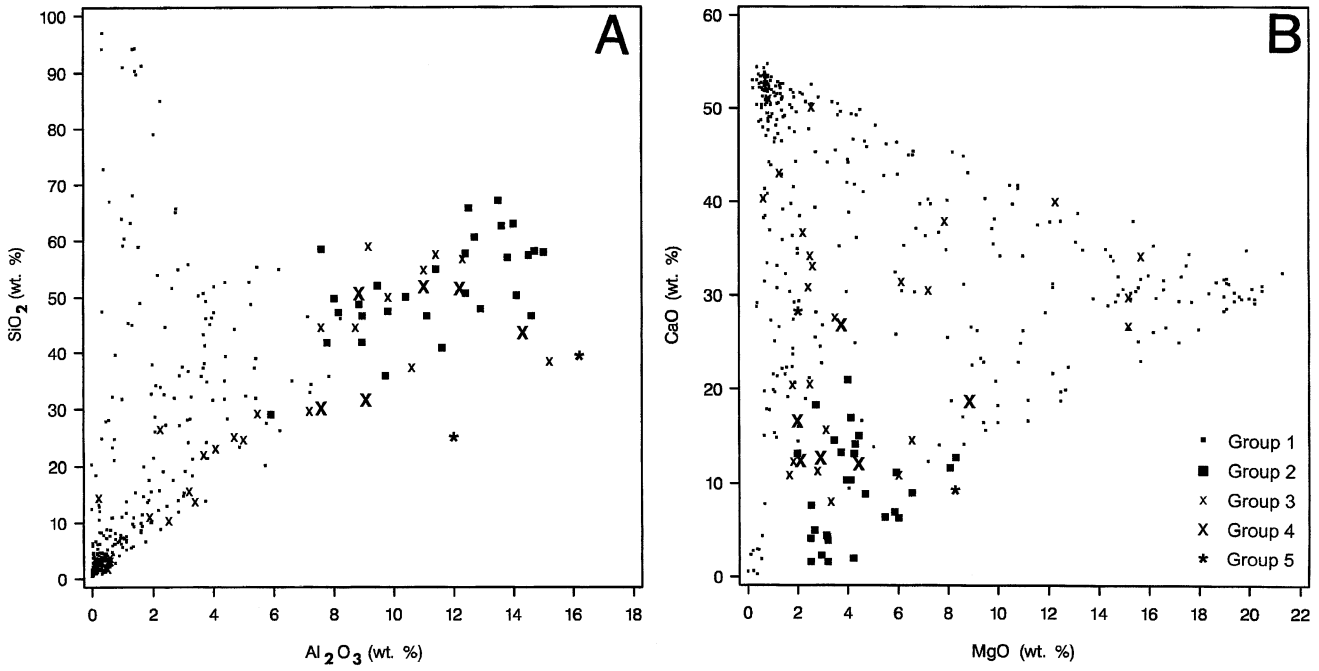

Figure 8. Comparison of major-element composition of different U-Th sample groups. Plotting symbols indicate sample groupings defined in Figure 7. In terms of these and most other major-element components, U-rich and U-poor groups are not well differentiated. (A) Bulk-rock silica vs. alumina. These components define a crude triangular plot having the following end members: spiculite (high-silicon [Si] apex), shale (high-Al apex), and carbonates (low–Si-Al apex). (B) Bulk-rock calcium oxide (CaO) vs. magnesium oxide (MgO). These components define a crude triangular plot having the following end members: limestone (high-Ca apex), dolomite (high-Mg apex), and siliciclastics or spiculite (low–Ca-Mg apex).

- Group 1 (336 samples) has low U (<12 ppm) and low Th (<6 ppm) and includes mainly limestones, dolostones, and spiculites.
- Group 2 (29 samples) has low U (<12 ppm U) and high Th (>6 ppm) and consists of shales and highly argillaceous limestones.
- Group 3 (25 samples) has high U (12–40 ppm) and low to high Th (<20 ppm).
- Group 4 (6 samples) has very high U (>40 ppm) and high Th. Both groups 3 and 4 include argillaceous carbonates and thin (0.5–5 cm) shale layers within carbonates. Groups 3 and 4 are believed to have similar geochemical significance (unusual uranium enrichment) except that group 4 represents the more extreme cases of enrichment.
- Group 5 (two samples) has very high Th (25–27 ppm) and includes one calcareous shale and one argillaceous limestone.

Various plots were examined to determine whether there were any other bulk chemical characteristics differentiating these U-Th groupings. We were especially interested to see what differences may exist corresponding to the difference in U enrichment between group 2 and groups 3 and 4. In terms of major element composition, these groups each show considerable variation and mutual overlap (Figure 8) except that ratios of both iron/aluminum (Fe/Al) and titanium/aluminum (Ti/Al) appear to correlate with the U enrichment differentiating group 2 from groups 3 and 4 (Figure 9).

SIGNIFICANCE OF K, Th, AND U ENRICHMENT

Potassium is interpreted as a simple index of bulk aluminosilicate content (clays, micas, and feldspars). Although not all aluminosilicate species are K rich, the aggregate assemblage of aluminosilicates present in these strata is distinctly K rich. Thorium, however, is not generally enriched in aluminosilicate minerals, but linear correlation of Th with K is nevertheless typical of siliciclastic strata (Schlumberger, 1982) and thus indicates a strong association between Th and aluminosilicates. Correlation between Th and zirconium (Zr) (Figure 10) suggests that this association may derive

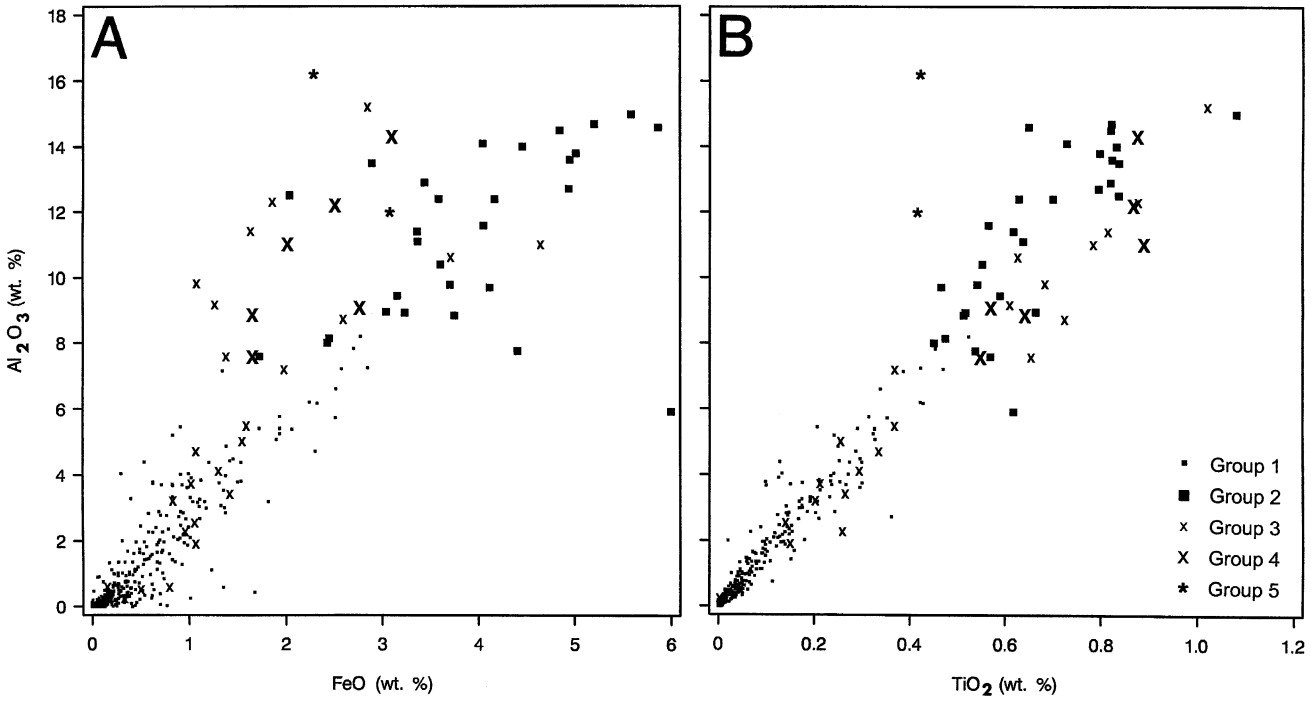

Figure 9. In contrast to most major elements (Figure 8), ratios of Fe and Ti to Al seem to separate U-rich from U-poor sample groups. Plotting symbols indicate sample groupings defined in Figure 7. (**A**) U-enriched samples (X) tend to be lower in bulk-rock iron content (total Fe as FeO) for given alumina content compared with low-U samples (filled squares). One sample having 16% FeO has been plotted at 6% FeO to increase plot scale. (**B**) U-enriched samples (X) tend to have slightly higher bulk-rock titanium for given alumina content compared with low-U samples (filled squares).

from the presence of Th in heavy minerals, such as zircon and monazite, which may be concentrated in low-energy (aluminosilicate-rich) siliciclastic facies due to fine particle size (Hurst and Milodowski, 1996). The proposed association between heavy mineral grains and aluminosilicates is also supported by the strong correlation observed between alumina and Ti, Ti being concentrated mainly as detrital rutile and ilmenite (Figure 9B). In previous spectral GR studies, wide variations in Th/K have been observed, having possible sequence stratigraphic and provenance significance (Myers and Wignall, 1987; Myers and Bristow, 1989; Davies and Elliott, 1996). In the present sample set, however, there is little variation in Th/K, with the notable exception of two Th-rich samples from GR peak 23 (Figure 6A), the significance of which is presently unknown.

Because U is typically uncorrelated with K and Th (Schlumberger, 1982; Figure 7), U content must be controlled by other factors in addition to aluminosilicate abundance. Based on the Th/U of an average of 67 mudrocks (3.8) (Adams and Weaver, 1958) and of the average crust (3.5) (Adams et al., 1959), Myers and Wignall (1987) suggested that there is a detrital (aluminosilicate-related) component of the total U content of shales, which is roughly equivalent to one-third of the total Th content. They considered the fraction of the bulk U exceeding one-third of the Th content to be authigenic U, interpreted to result from synsedimentary U fixation at the sediment-water interface due to sorption on organic matter under anoxic conditions. Nearly all of the 7128/6-1 samples, including many of the low-U Group-2 shales, have Th/U less than 3 (Figure 7). The average Th/U of the 398 samples analyzed is 2.07/5.04 = 0.41. Thus most of the U in these Carboniferous–Permian strata is nondetrital in origin.

Uranium-enriched shales elsewhere have generally been interpreted as reflecting slow accumulation of organic-rich marine sediments under deep-water, oxygen-poor conditions (Swanson, 1961; Myers and Wignall, 1987; Saller et al., 1994). This seems unlikely for the U-rich zones in the 7128/6-1 section, however, which correspond to either thin clay layers in shallow-water carbonate facies or relatively minor transgressive events (shaly carbonates) that mark the basal zones of

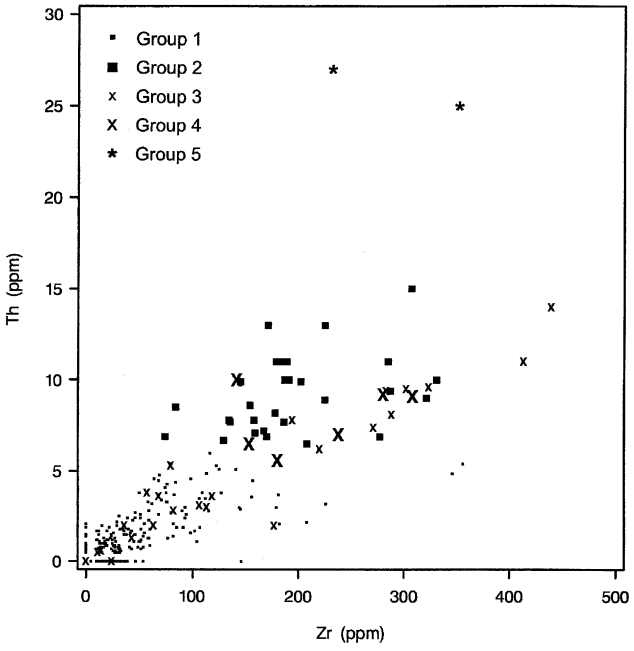

Figure 10. Bulk-rock Th vs. Zr in Moscovian through Upper Permian samples (units L-1 through L-9) from well 7128/6-1. Plotting symbols indicate sample groupings defined in Figure 7. Correlation between these elements (and also correlation between Th and Ti; implicit in the alumina-Ti correlation shown in Figure 9B) supports the interpretation that Th is contained mainly in heavy mineral grains, such as zircon and monazite.

high-order depositional cycles. The clearest candidate in the 7128/6-1 section for oxygen-poor conditions of sedimentation is a 1 m zone of moderately organic-rich shale (total organic carbon = 0.7–2.7 at a vitrinite reflectance level of 0.6% R_o) at the base of unit L-9 (high-GR interval 32 in Figure 2), but these samples have low U (3–5 ppm). Correlation between U and organic carbon is typical of U-enriched sediments deposited under oxygen-poor conditions (Swanson, 1960; Schlumberger, 1982; Myers and Wignall, 1987). No such correlation is observed in the present data set, but this question cannot be properly evaluated at present because total organic carbon was not analyzed for any of the samples having U > 22 ppm.

Rather than marine anoxia, U-enrichment in the 7128/6-1 strata appears to be associated with shallow-water carbonate environments probably having oxygen-rich conditions, as indicated by near complete absence of pyrite and many surfaces of inferred subaerial exposure. To account for this association, we suggest that U may have been concentrated by groundwater oxidation-reduction processes on the exposed platform surface during lowstands of sea level. Uranium is much more soluble in its oxidized (VI) state than in its reduced (IV) state, resulting in U mobility in oxidized groundwater followed by fixation and accumulation in the vicinity of reducing conditions associated with decaying organic matter (Hostetler and Garrels, 1962; Doi et al., 1975; Langmuir, 1978). Subsequent minor flooding events could then have caused reworking of U-enriched argillaceous detritus and deposition as thin shale layers.

Larger degrees of subaerial exposure of the siliciclastic fraction contributing to the U-enriched samples is consistent with the tendency of these samples to have lower Fe/Al and higher Ti/Al compared with the low-U samples (Figure 9), insofar as Fe is relatively soluble and Ti is relatively insoluble relative to Al during subaerial weathering (Gardner, 1980).

A similar model was proposed by Hoff et al. (1995, p. 226) for accumulation of U to form "hot dolostones" at a major unconformity in the Upper Carboniferous Wahoo formation, Alaska. Lead isotopic dating shows that U enrichment coincided with formation of this unconformity in the middle Permian. As in the 7128/6-1 strata, U in the Wahoo dolostones is concentrated in thin clay-rich layers rather than in the enclosing carbonate rock. Hassan et al. (1975) described similar relationships in Nummulitic Eocene limestones, Tunisia, where spectral GR signature is dominated by thin, highly U-enriched shale seams in otherwise U-poor limestone.

Other examples of U-rich spectral GR peaks in carbonates have been suggested to result from late diagenetic fluid movements. Fertl et al. (1980) presented spectral GR profiles from the Cretaceous Austin Chalk, Texas, where the coincidence of U-rich, K-Th–poor zones with good petroleum production characteristics was viewed as evidence for late diagenetic precipitation of U in fractures. Luczaj (1998) showed spectral GR logs from carbonate-siliciclastic cycles of the lower Permian Chase Group, Kansas, where U peaks occur within the carbonates and Th-K peaks correspond to siltstone-shale units, not unlike the overall pattern of U-Th-K distribution in well 7128/6-1. U enrichment in the Chase Group, however, was interpreted to have been a late diagenetic process related to dolomitization.

PROVENANCE

Based on the preceding arguments, high U/Th compositions in well 7128/6-1 are interpreted as reflecting

derivation of aluminosilicate detritus from surfaces of extended subaerial exposure where shallow meteoric groundwater movements had caused U enrichment. At the other extreme, shales having low U/Th are viewed as the products of relatively major marine transgressions, during which much of the aluminosilicate detritus was derived from sources not affected by the presumed process of subaerial U enrichment. None of these transgressions (at least in the inner-platform position of well 7128/6-1) seem to have involved anoxic accumulation of U-enriched organic matter, analogous to the phosphatic core shales that represent maximum-flooding events of the more principal cyclothems of the mid-continent United States (Heckel, 1977; Saller et al., 1994).

The reason for the apparent lack of aluminosilicate derivation from U-enriched provenance during major transgressions is unknown. A possible explanation is that U mineralization took place mainly on the exposed platform surface, and this surface was simply not available as a source of aluminosilicate detritus during major transgressions because it was then below sea level. During these transgressions, detritus would have been derived more directly from highlands nearer the interior of the Fennoscandian craton, where groundwater mobilization of U may have been less efficient because of differing hydrologic regimes. Another possibility is that sea level lowstands may have been associated with periods of relatively arid climate, whereas transgressions were associated with a more humid climate, as has been documented for Upper Carboniferous–Permian cycles in the western United States (Rankey, 1997; Soreghan, 1997). Arid conditions could favor U mineralization due to evaporative focusing of groundwater flow toward the surface (Rawson, 1980).

The preceding model does not necessarily imply that there should be any fundamental difference in siliciclastic provenance between U-dominated and K-Th–dominated intervals. The essential difference between these two categories is interpreted to be the degree of secondary enrichment in U, and this can be entirely a function of residence time on the exposed platform surface rather than the nature or location of the terranes eroded to produce the siliciclastic detritus. The absence of any consistent difference in primary provenance between U-enriched and non–U-enriched intervals is indicated by a profile of samarium (Sm)-neodymium (Nd) isotopic analyses acquired through the 7128/6-1 section (Ehrenberg et al., 2000b). Shifts in Nd provenance signature ($^{143}Nd/^{144}Nd$) appear to have a much larger scale cyclicity than the variation between K-Th–rich and U-rich compositions. Unfortunately, however, this question can only be evaluated rather indirectly, because none of the samples from the present article having especially high U/Th were selected for Nd isotopic analysis. Nevertheless, the Nd sample set does include samples from the K-Th–dominated transgressive shale intervals and samples from adjacent carbonate intervals having U-dominated GR peaks (sample points located between the thin U-enriched layers), and comparison of these two sample settings does not reveal consistent differences in $^{143}Nd/^{144}Nd$.

CONCLUSIONS

Our model predicts that K-Th–dominated GR peaks, such as those that occur in units L-1, L-2, and L-7, are the products of relatively major marine transgressions (aluminosilicate detritus derived mainly from sources inland of the platform surface), whereas the U-dominated GR peaks, such as those that characterize units L-3 through L-5, reflect more minor transgressions (aluminosilicate detritus derived mainly by reworking the subaerially exposed platform surface).

The composite low-U/Th over high-U/Th structure of most of the K-Th–dominated GR peaks in well 7128/6-1 is interpreted to indicate abrupt cycling from minimum to maximum accommodation conditions. The basal, high-U/Th part of the GR peak reflects multiple exposure and minor flooding events during late highstand. The upper, low-U/Th part of the GR peak reflects transgression. Similar regressive-transgressive turnaround is also represented in the U-dominated GR peaks, but the distinctive K-Th–dominated transgressive shale zone is less clearly developed.

The results of this study are potentially useful for petroleum exploration in frontier provinces where little may be known about the carbonate strata penetrated by initial drilling. Although spectral GR signatures alone would not provide conclusive interpretations of depositional history, this type of evidence could nevertheless be of value to the overall evaluation. Uranium-dominated GR peaks should be considered as possibly indicating the influence of extended subaerial exposure: either the presence of an exposure surface or the presence of sediment derived by erosion and resedimentation from an exposed platform top. Care must be taken, however, to evaluate whether the Finnmark Platform example is relevant to

other provinces and also to avoid confusing U-dominated GR signatures related to subaerial exposure with possibly similar signatures related to deep-water anoxic sedimentation or late diagenetic fluid movement.

REFERENCES CITED

Adams, J. A. S., and R. Weaver, 1958, Thorium-to-uranium ratio as an indicator of sedimentary process: examples of the concept of geochemical facies: AAPG Bulletin, v. 42, p. 387–430.

Adams, J. A. S., J. K. Osmund, and J. J. W. Rogers, 1959, The geochemistry of uranium and thorium: Physical Chemistry of the Earth, v. 3, p. 299–328.

Beauchamp, B., and A. Desrochers, 1997, Permian warm- to very cold-water carbonates and cherts in northwest Pangea, *in* N. P. James and J. A. D. Clarke, eds., Cool-water carbonates: SEPM Special Publication 56, p. 327–347.

Davies, S. J., and T. Elliott, 1996, Spectral gamma ray characterization of high resolution sequence stratigraphy: examples from Upper Carboniferous fluvio-deltaic systems, County Clare, Ireland, *in* J. A. Howell and J. F. Aitken, eds., High resolution sequence stratigraphy: innovations and applications: Geological Society Special Publication 104, p. 25–35.

Doi, K., H. Shuichiro, and Y. Sokamaki, 1975, Uranium mineralization in groundwater in sedimentary rocks, Japan: Economic Geology, v. 70, p. 628–646.

Dypvik, H., and D. Ø. Eriksen, 1983, Natural radioactivity of clastic sediments and the contributions of U, Th and K: Journal of Petroleum Geology, v. 5, p. 409–416.

Ehrenberg, S. N., and E. Siring, 1992, Use of bulk chemical analyses in stratigraphic correlation of sandstones: an example from the Statfjord Nord field, Norwegian continental shelf: Journal of Sedimentary Petrology, v. 62, p. 318–330.

Ehrenberg, S. N., E. B. Nielsen, T. A. Svånå, and L. Stemmerik, 1998a, Depositional evolution of the Finnmark carbonate platform, Barents Sea: results from wells 7128/6-1 and 7128/4-1: Norsk Geologisk Tidsskrift, v. 78, p. 185–224.

Ehrenberg, S. N., E. B. Nielsen, T. A. Svånå, and L. Stemmerik, 1998b, Diagenesis and reservoir quality of the Finnmark carbonate platform, Barents Sea: results from wells 7128/6-1 and 7128/4-1: Norsk Geologisk Tidsskrift, v. 78, p. 225–251.

Ehrenberg, S. N., N. A. H. Pickard, T. A. Svånå, I. Nilsson, and V. I. Davydov, 2000a, Sequence stratigraphy of the inner Finnmark carbonate platform (Upper Carboniferous–Permian), Barents Sea—correlation between well 7128/6-1 and the shallow IKU cores: Norsk Geologisk Tidsskrift, 80, p. 129–161.

Ehrenberg, S. N., T. A. Svånå, B. Patterson, and E. W. Mearns, 2000b, Neodymium isotopic profiling of carbonate platform strata: correlation between siliciclastic provenance signature and sequence stratigraphy: Sedimentary Geology, v. 131, p. 87–95.

Fertl, W. H., W. L. Stapp, D. B. Vaello, and W. C. Vercellino, 1980, Spectral gamma-ray logging in the Austin Chalk trend: Journal of Petroleum Technology, v. 32, p. 481–488.

Gardner, L. R., 1980, Mobilization of Al and Ti during weathering—isovolumetric chemical evidence: Chemical Geology, v. 30, p. 151–165.

Hassan, M., M. Selo, and A. Combaz, 1975, Uranium distribution and geochemistry as criteria of diagenesis in carbonate rocks: IX Congres International de Sedimentologie, Nice, France, v. 7, p. 69–75.

Hassan, M., A. Hossin, and A. Combaz, 1976, Fundamentals of the differential gamma ray log—interpretation technique: Society of Professional Well Log Analysts 17th Annual Logging Symposium Transactions, paper H, 18 p.

Heckel, P. H., 1977, Origin of phosphatic black shale facies in Pennsylvanian cyclothems of mid-continent North America: AAPG Bulletin, v. 61, p. 1045–1068.

Hoff, J. A., J. Jameson, and G. N. Hanson, 1995, Application of Pb isotopes to the absolute timing of regional exposure events in carbonate rocks: an example from U-rich dolostones from the Wahoo formation (Pennsylvanian), Prudhoe Bay, Alaska: Journal of Sedimentary Research, v. A65, p. 225–233.

Hostetler, P. B., and R. M. Garrels, 1962, Transport and precipitation of uranium and vanadium at low temperatures, with special reference to sandstone-type uranium deposits: Economic Geology, v. 57, p. 137–167.

Hurst, A., and Milodowski, A., 1996, Thorium distribution in some North Sea sandstones: implications for petrophysical evaluation: Petroleum Geoscience, v. 2, p. 59–68.

Langmuir, D., 1978, Uranium solution—mineral equilibria at low temperatures with applications to sedimentary ore deposits: Geochimica et Cosmochimica Acta, v. 42, p. 547–569.

Larssen, G. B., G. Elvebakk, L. B. Henriksen, S. E. Kristensen, I. Nilsson, T. J. Samuelsberg, and T. A. Svånå, 1999, Lithostratigraphical nomenclature of the Upper Paleozoic rocks of the southwestern Barents Sea: Geonytt, January issue, p. 65.

Lucia, F. J., 1999, Carbonate reservoir characterization: Berlin, Springer-Verlag, 226 p.

Luczaj, J. A., 1998, Regional stratigraphic distribution of uranium in the Lower Permian Chase Group carbonates of southwestern Kansas: The Log Analyst, v. 39, p. 18–26.

Myers, K. J., and C. S. Bristow, 1989, Detailed sedimentology and gamma-ray log characteristics of a Namurian deltaic succession II: gamma-ray logging, *in* M. K. G. Whateley and K. T. Pickering, eds., Deltas: sites and traps for fossil fuels: Geological Society Special Publication 41, p. 81–88.

Myers, K. J., and P. B. Wignall, 1987, Understanding Jurassic organic-rich mudrocks—new concepts using gamma-ray spectrometry and palaeoecology: examples from the Kimmeridge Clay of Dorset and the Jet Rock of Yorkshire, *in* J. K. Legget and G. G. Zuffa, eds., Marine clastic sedimentology: London, Graham and Trotman, p. 172–189.

North, C. P., and M. Boering, 1999, Spectral gamma-ray logging for facies discrimination in mixed fluvial-eolian successions: a cautionary tale: AAPG Bulletin, v. 83, p. 155–169.

Pickard, N. A. H., F. Eilertsen, N.-M. Hanken, T. A. Johansen, A., Lønøy, H. A. Nakrem, I. Nilsson, T. J. Samuelsberg, and I. D. Somerville, 1996, Stratigraphic framework of Upper Carboniferous (Moscovian–Kasimovian) strata in Bünsow Land, central Spitsbergen: palaeogeographic implications: Norsk Geologisk Tidsskrift, v. 76, p. 169–185.

Rankey, E. C., 1997, Relations between relative changes in sea level and climate shifts: Pennsylvanian–Permian mixed carbonate-siliciclastic strata, western United States: Geological Society of American Bulletin, v. 109, p. 1089–1100.

Rawson, R. R., 1980, Uranium in the Jurassic Todilto Limestone of New Mexico—an example of a sabkha-like deposit, *in* C. E. Turner-Peterson, ed., Uranium in sedimentary rocks: application of the facies concept to exploration: SEPM Short Course Notes, p. 127–147.

Saller, A. H., J. A. D. Dickson, and S. A. Boyd, 1994, Cycle stratigraphy and porosity in Pennsylvanian and Lower Permian shelf limestones, eastern Central Basin platform, Texas: AAPG Bulletin, v. 78, p. 1820–1842.

Schlumberger, 1982, Natural gamma-ray spectrometry: essentials of N. G. S. interpretation: Schlumberger, 69 p.

Shinn, E. A., 1986, Modern carbonate tidal flats: their diagnostic features: Colorado School of Mines Quarterly, v. 81, p. 7–35.

Soreghan, G. S., 1997, Walther's Law, climate change, and Upper Paleozoic cyclostratigraphy in the Ancestral Rocky Mountains: Journal of Sedimentary Research, v. 67, p. 1001–1004.

Stemmerik, L., and G. B. Larssen, 1993, Diagenesis and porosity evolution of Lower Permian *Palaeoaplysina* build-ups, Bjørnøya: an example of diagenetic response to high frequency sea level fluctuations in an arid climate, *in* A. D. Horbury and A. D. Robinson, eds., Diagenesis and basin development: AAPG Studies in Geology 36, p. 199–211.

Stemmerik, L., and D. Worsley, 1995, Permian history of the Barents Sea area, *in* P. A. Scholle and T. M. Peryt, eds., Permian of the northern continents: Berlin, Springer-Verlag, p. 81–97.

Swanson, V. E., 1960, Oil yield and uranium content of black shales: U.S. Geological Survey Professional Paper 356-A, 44 p.

Swanson, V. E., 1961, Geology and geochemistry of uranium in marine black shales, a review: U.S. Geological Survey Professional Paper 356-C, p. 67–112.

Veevers, J. J., and C. M. C. A. Powell, 1987, Late Paleozoic glacial episodes in Gondwanaland reflected in transgressive-regressive depositional sequences in Euramerica: Geological Society of America Bulletin, v. 98, p. 475–487.